Journal of Applied Physics

RESEARCH ARTICLE | AUGUST 23 2019

First-principles study of coupled effect of ripplocations and S-vacancies in MoS_2 FREE

Georgios A. Tritsaris; Mehmet Gökhan Şensoy; Sharmila N. Shirodkar; Efthimios Kaxiras

Journal of Applied Physics 126, 084303 (2019)
https://doi.org/10.1063/1.5099496

CHORUS

CrossMark

Downloaded from http://pubs.aip.org/aip/jap/article-pdf/doi/10.1063/1.5099496/13866432/084303_1_online.pdf

Journal of Applied Physics | ARTICLE | scitation.org/journal/jap

First-principles study of coupled effect of ripplocations and S-vacancies in MoS_2

Cite as: J. Appl. Phys. **126**, 084303 (2019); doi: 10.1063/1.5099496
Submitted: 10 April 2019 · Accepted: 5 August 2019 ·
Published Online: 23 August 2019

View Online

Export Citation

CrossMark

Georgios A. Tritsaris,[1,2,a)] Mehmet Gökhan Şensoy,[3,a)] Sharmila N. Shirodkar,[1,a),b)] and Efthimios Kaxiras[1,4,c)]

AFFILIATIONS

[1]John A. Paulson School of Engineering and Applied Sciences, Harvard University, Cambridge, Massachusetts 02138, USA
[2]Institute for Applied Computational Science, Harvard University, Cambridge, Massachusetts 02138, USA
[3]Department of Physics, Recep Tayyip Erdogan University, 53000 Rize, Turkey
[4]Department of Physics, Harvard University, Cambridge, Massachusetts 02138, USA

[a)]**Contributions:** G. A. Tritsaris, M. G. Şensoy, and S. N. Shirodkar contributed equally to this work.
[b)]**Present address:** Department of Materials Science and NanoEngineering, Rice University, Houston, Texas 77005, USA.
[c)]**Author to whom correspondence should be addressed:** kaxiras@physics.harvard.edu

ABSTRACT

Recent experiments have revealed ripplocations, atomic-scale ripplelike defects on samples of MoS_2 flakes. We use quantum mechanical calculations based on density functional theory to study the effect of ripplocations on the structural and electronic properties of single-layer MoS_2, and, in particular, the coupling between these extended defects and the most common defects in this material, S-vacancies. We find that the formation of neutral S-vacancies is energetically more favorable in the ripplocation. In addition, we demonstrate that ripplocations alone do not introduce electronic states into the intrinsic bandgap, in contrast to S-vacancies. We study the dependence of the induced gap states on the position of the defects in the ripplocation, which has implications for the experimental characterization of MoS_2 flakes and the engineering of quantum emitters in this material. Our specific findings collectively aim to provide insights into the electronic structure of experimentally relevant defects in MoS_2 and to establish structure-property relationships for the design of MoS_2-based quantum devices.

Published under license by AIP Publishing. https://doi.org/10.1063/1.5099496

I. INTRODUCTION

In materials, crystal defects and impurities play a crucial role in determining the mechanical, thermal, electronic, and optical properties of materials, and two-dimensional (2D) materials are no exception to this rule.[1–6] The nature of defects that form due to ambient contamination depend on growth conditions such as temperature, pressure, and concentration of constituent elements. Experimental samples can be characterized on the basis of the signature of defects in measured spectra when reliable reference information is available about the structural and electronic properties of the material. Moreover, strain and defect engineering constitute common strategies for modifying materials properties toward tailored functionality for their use as active components in devices. The approach relies on a detailed understanding of the (often nontrivial) relationship between strain and defects in the material and how they affect its electronic properties.

Transition metal dichalcogenides (TMDCs), such as MoS_2, are a class of 2D layered materials. The general stability of TMDCs, their mechanical flexibility, and relatively inexpensive production, together with a bandgap suitable for optical applications make them excellent candidates for active materials in electronic devices,[7–10] including quantum emitters,[11] with advantages over bulk materials.[12–14]

MoS_2 is a semiconductor with a bandgap of 1.9 eV as a single layer and 1.3 eV in bulk form. Detailed experimental[4,15,16] and theoretical[5,17] studies of different types of defects in MoS_2 have revealed chalcogen atom vacancies (S-vacancies) to be the most common defect.[6,18–20] Such defects introduce states in the bandgap of the semiconductor, which alter its photoluminescence (PL) and cathodoluminescence (CL) spectra.[4,19,21] S-vacancies are speculated to give MoS_2 its intrinsic "n" type character.[15,22] A different type of extended, one-dimensional defect are ripplocations; these occur when one layer slips against another, creating a line defect with the dual character of an atomic-scale ripple and a crystallographic dislocation. These defects are topologically identical but energetically different than dislocation defects in bulk materials. Unlike same-

Downloaded from http://pubs.aip.org/aip/jap/article-pdf/doi/10.1063/1.5099496/13866432/084303_1_online.pdf

sign dislocations which repel each other according to Frank's superlinear energy scaling rule, ripplocations attract one another to form larger immobile folds when they merge.[23] Exfoliation of MoS_2, used to isolate individual layers of the material, has been reported to give rise to ripplocations.[19,23]

Experimental work by Fabbri *et al.*[19] has suggested an emission peak observed at 0.98 eV in the CL spectrum of MoS_2 flakes to be the signature of ripplocations, although the evidence was inconclusive. Because interpretation of measured properties often relies on assumptions regarding the response of the material, theory and atomistic simulation have contributed significantly in clarifying how the properties of MoS_2 and other layered semiconductors depend on atomic-scale structural features. Ostadhossein *et al.*[24] estimated the formation energy of S-vacancies with respect to the local curvature of the ripplocation in bilayers of the material, and studied their diffusion across the ripplocation using reactive force fields (ReaxFF with multiple energy contributions). Kushima *et al.*[23] used stoichiometric structural models and density functional theory (DFT) calculations to explain findings from transmission electron microscopy for ripplocations on MoS_2 crystals. Materials modeling has also been used to elucidate the nature of localized defects and associated single photon emission in the atom-thick hBN.[25] However, the effect of ripplocations on the structural and electronic properties, including photon emission, of S-deficient forms of MoS_2 remain largely unexplored.

Here, we carry out first-principles calculations based on DFT to study the trends in the structural and electronic properties of model S-deficient structures of a single layer of MoS_2 with a ripplocation. We calculate induced strain in the structures, and the dependence of the defect-induced states in the bandgap on the position of point and line defects in the ripplocation, in order to obtain insights into the coupling of ripplocations with S-vacancies. In contrast to previous work, we use first-principles calculations to study extended S-deficient forms of free-standing layers of MoS_2 and specifically the limiting cases of isolated point defects and extended line defects perpendicular to the ripplocation. While this class of defects are the primary focus of our work, we anticipate that our findings will also help rationalize experiments on other types of defects in layered MoS_2, such as flake edges, by providing reliable reference information for the interpretation of the material's optoelectronic response in terms of individual contributions from each class of defects.

II. METHODS

We used a rectangular unit cell consisting of two Mo and four S atoms in order to model a single flat layer of MoS_2 with empty space of 15 Å on each side. The choice of empty regions was guided by the requirement that the wavefunctions vanish smoothly at the edge of the unit cell, as would be required in a model of an isolated layer. To model ripplocations, we used 14×2 supercells that were compressed along the direction of the armchair edge by 5% before the structural model was optimized with fixed positions of the atoms far from the ripplocation center (Fig. 1). Different initial shapes for the ripplocation were used for structural optimization to avoid metastable structures, including sinusoidal and Gaussian forms. Monolayers with isolated S-vacancies were modeled by removing one or two S atoms in either the top or bottom atomic layer to create a single vacancy or a pair of S-vacancies in one of three different parts (or segments) of the ripplocation (Segments I, II, and III in Fig. 1). These point defects are separated from the center of the ripplocation by about 7 Å, 14 Å, and 22 Å for Segments I, II, and III, respectively, and by 6.4 Å from their mirror image along the zigzag direction. Four S-vacancies were used to model a pair of extended lines of defects (one line on each side of the ripplocation) by removing the remaining two S atoms along the zigzag direction adjacent to the defects in the model structures with two S-vacancies.

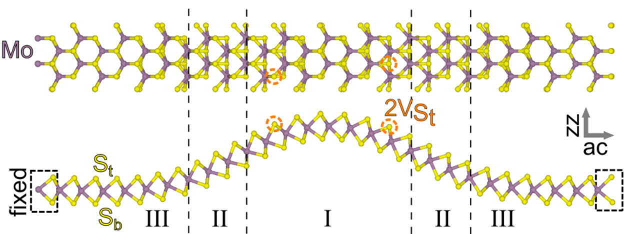

FIG. 1. Top and side views of the structural model of a stoichiometric single layer of MoS_2 with a ripplocation along the armchair (ac) direction (zz for zigzag). Purple and yellow balls represent Mo and S atoms, respectively. I, II, and III indicate three segments of the single layer with different local ripplocation curvatures. Orange circles mark the position of a pair of S-vacancies in the top atomic layer ($2V_{S_t}$) of Segment I.

Electronic structure calculations were carried out using the Quantum ESPRESSO package.[26] The interaction between the ions and electrons was described using Ultrasoft pseudopotentials[27] and a plane wave basis set with a cutoff of 30 Ry was used to represent the Kohn-Sham wavefunctions. For the description of exchange and correlation, the Perdew-Burke-Ernzerhof (PBE)[28] functional was chosen, although we do not expect the general trends identified in this study to depend sensitively on the functional. The Brillouin zone was sampled using a 1×2 Monkhorst-Pack reciprocal-space lattice. For structural optimization, the atomic configurations were relaxed by the minimization of the magnitude of all interatomic forces with an upper limit of 0.025 eV/Å.

III. RESULTS AND DISCUSSION

We begin by investigating the effect of the ripplocation on the properties of the stoichiometric single layer of MoS_2. The structural model of rippled layer is shown in Fig. 1. Because the layer is strained, it buckles out of the plane in order to reduce compressive stress. The buckling height is 8.1 Å, calculated as the projection of the displacement on the direction perpendicular to the layer of the separation between two Mo atoms nearest and farthest from the ripplocation center. The residual strains are shown in Fig. 2 pertaining to the bonds between Mo (labeled as "Mo–Mo"), and Mo and S ("Mo$-S_t$" and "Mo$-S_b$"). The effect of the ripplocation on the distance between S atoms on the opposite sides of the Mo sublayer is also shown ("S_t-S_b"). These bonds and distances are found to be strained near the center of the ripplocation (Fig. 2), compressed by 0.5% and 0.8% for Mo–Mo and Mo$-S_b$, and stretched by 0.5% and 0.3% for Mo$-S_t$ and S_t-S_b, respectively. We calculate larger strain

Downloaded from http://pubs.aip.org/aip/jap/article-pdf/doi/10.1063/1.5099496/13866432/084303_1_online.pdf

Published under license by AIP Publishing.

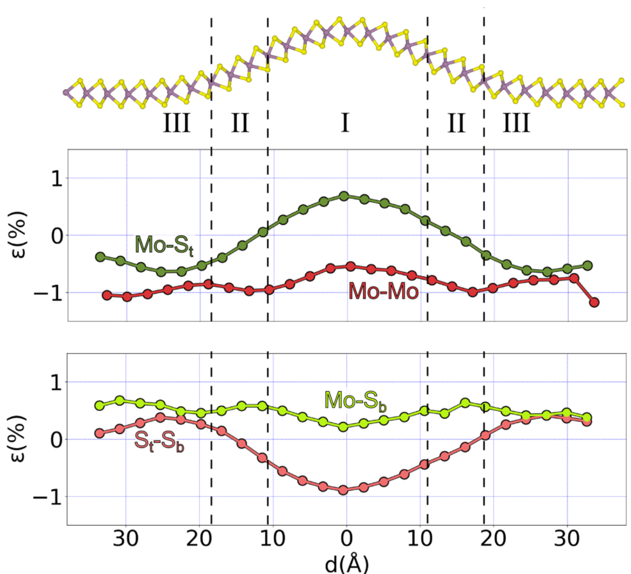

FIG. 2. Strain, ϵ, acting on the layer of MoS_2 due to the ripplocation, measured in terms of the separation between Mo atoms, and between Mo and S atoms (S_t for the top and S_b for the bottom atomic layer of sulfur). Zero denotes the position of the center of the ripplocation.

than that reported in Kushima *et al.*[23] (<0.1%) for similar simulation parameters and model size, although here we model a single layer, as opposed to the bilayer in the aforementioned work.

Though the formation of S-vacancies has been studied previously,[4,5,17] their interaction with ripplocation defects has been considered only recently.[24] We carry out a detailed analysis of their coupling by introducing one S-vacancy ($1V_S$), a pair of S-vacancies ($2V_S$), or a pair of lines of S-vacancies ($4V_S$) in the top [$(1, 2, 4)V_{S_t}$] or bottom atomic layer [$(1, 2, 4)V_{S_b}$], i.e., the convex or concave surface of the ripplocation, with increasing separation from its center or decreasing ripplocation curvature in their vicinity (Segments I, II and III in Fig. 1). $1V_S$, $2V_S$, and $4V_S$ correspond to a concentration of 1.8%, 3.6%, and 7.2% in the atomic layer of sulfur. In the following, we discuss the changes in the structure and electron density of states that the S-vacancies induce.

A. Defect formation

First, we examine whether the formation of S-vacancies in the ripplocation is energetically favorable. We calculate the formation energy per S-vacancy, E_f, as

$$E_f(n) = \frac{E_V(n) - E_{st} + nE_S}{n},$$

where E_V is the total energy of the S-deficient rippled single layer, E_{st} is the energy of the stoichiometric layer, E_S is the energy per S atom in a S_8 molecule in the gas phase, and n is the number of S-vacancies in the 14×2 simulation cell (n = 1, 2, 4). More positive formation energies indicate energetically less favorable formation of

TABLE I. Formation energies per S-vacancy, ΔE_F (in eV), and change in buckling height of the ripplocation, Δh (in Å), for a single vacancy (1), a pair of isolated vacancies (2), or a pair of lines of vacancies (4) in the rippled MoS_2 supercell.

	V_{S_t}			V_{S_b}		
	I	II	III	I	II	III
$\Delta E_F(1)$	2.19	1.88	1.89	1.41	1.73	1.82
$\Delta E_F(2)$	2.79	2.61	2.36	2.24	2.29	2.55
$\Delta E_F(4)$	1.99	2.58	1.61	1.76	1.58	2.28
$\Delta h(1)$	0.62	1.36	0.41	0.90	0.12	0.91
$\Delta h(2)$	−0.41	−0.88	−1.10	−0.83	0.31	0.94
$\Delta h(4)$	−0.81	−0.36	−1.18	−1.42	−1.31	0.11

defects with respect to the above two reference states. Using the above expression, the formation energies of $1V_{S_t}$ are calculated to be in the range of 1.41–2.19 eV (Table I). The position of the S-vacancies is shown in the structural model of Fig. 3. The formation energy of $1V_{S_t}$ decreases as its distance from the ripplocation center increases, or equivalently, with decreasing curvature of ripplocation locally, which is in agreement with previous studies based on DFT.[24] The formation energy of $1V_{S_b}$ shows the opposite trend. The deviation between the formation energies is maximized near the center of the ripplocation (Segment I), whereas they converge far from it (III), as would be expected, since the top and bottom layers become equivalent in this limit. S-vacancies are, therefore, more likely to form in a ripplocation: compare the calculated formation energies for $1V_{S_b}$ near the center of the ripplocation and far from it.

The ripplocation in the presence of a single S-vacancy undergoes deformation that involves asymmetric bending toward the point defect. In this case, separating the contribution of the isolated S-vacancies and the ripplocation to local structural deformation becomes nontrivial. To circumvent this issue, we study the effect of a pair of S-vacancies, one at each side of the ripplocation and roughly at the same separation from its center, within each Segment (Fig. 3). The formation energies for a pair of S-vacancies are summarized in Table I: they decrease for $2V_{S_t}$ and increase for $2V_{S_b}$ with decreasing curvature of the ripplocation, being in the range of 2.24–2.79 eV and following the same trend as for $1V_S$.

We also examine the case of a pair of extended lines of S-vacancies, perpendicular to the ripplocation (i.e., along the zigzag direction). Their formation energies are calculated to be in the range between 1.58 eV and 2.58 eV per S atom. We use two pairs of lines, one at each side of the ripplocation as in the case of a pair of S-vacancies, to avoid contributions of asymmetric bending of the rippled layer. A trend in formation energies is less clear for $4V_S$ although on average, they are found to be lower than those associated with $2V_S$ by 0.50 eV. The calculations indicate that it is energetically favorable for S-vacancies to concentrate near the ripplocation [see $4V_{S_b}$(II) in Table I] and suggest strain as a means for moving them.

B. Strain effects

The change in strain, $\Delta\epsilon$, in the S-deficient structure with one S-vacancy in the top atomic layer (the convex surface of the ripplocation) with respect to the stoichiometric rippled layer is shown in

Downloaded from http://pubs.aip.org/aip/jap/article-pdf/doi/10.1063/1.5099496/13866432/084303_1_online.pdf

Published under license by AIP Publishing.

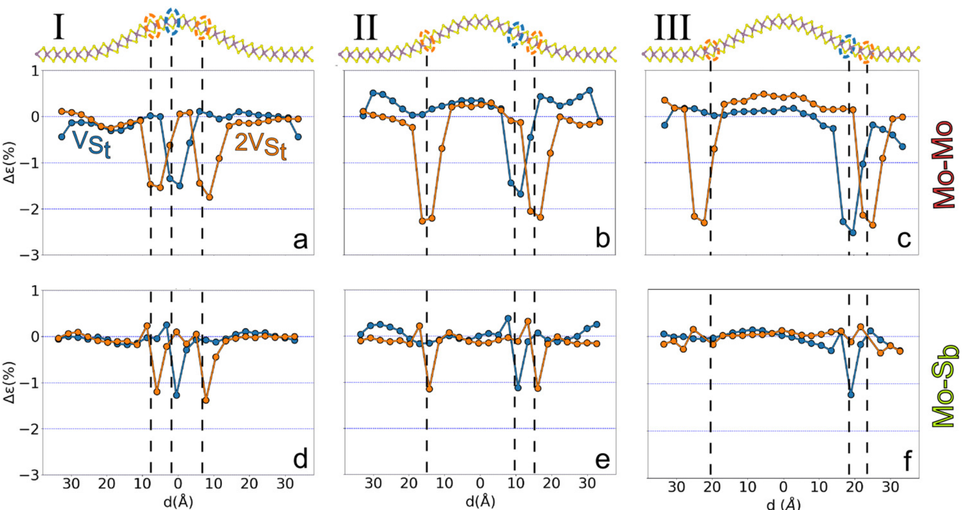

FIG. 3. Change in strain, $\Delta\epsilon$, in the presence of a single S-vacancy (blue, $1V_{S_t}$) or a pair of vacancies (orange, $2V_{S_t}$) in the top atomic layer of MoS_2 with respect to the stoichiometric form (see also Fig. 2). (a)–(c) Effect of strain on the bond between Mo atoms; (d)–(f) effect of strain on the bond between Mo and S in the bottom atomic layer of the MoS_2. The position of the defects along the armchair direction is marked using dashed lines. Zero (0) on the x axis denotes the position of the center of the ripplocation.

Downloaded from http://pubs.aip.org/aip/jap/article-pdf/doi/10.1063/1.5099496/13866432/084303_1_online.pdf

Fig. 3 for the Mo–Mo and Mo–S_b bonds. We find that bonds near the S-vacancies generally experience an increased amount of compressive strain, and both Mo–Mo and Mo–S_b bonds are compressed.

For $1V_{S_t}$, we find that the Mo–Mo bond compresses by 1.5% (2.4% for $1V_{S_b}$) in Segment I, by 1.7% (2.6%) in Segment II, and by 2.5% (2.0%) in Segment III. The bonds between Mo and S atoms in the concave surface of ripplocation (Mo–S_b) compress but vary less with respect to the separation of the vacancies from the center of ripplocation, being in the range of 1.1%–1.3%. The effect is almost absent for $1V_{S_b}$. The trends in Mo–S_t and Mo–S_b are reversed between $1V_{S_t}$ and $1V_{S_b}$. Little variation is found for the S_t–S_b separation, which expands by no more than 0.5% near the S-vacancies. Similarly, the height of the ripplocation (or buckling height) is also altered by the S-vacancies (see Table I).

The trends in strain for a pair of S-vacancies or a pair of lines of S-vacancies are similar to those for a single S-vacancy. For instance, we find that the maximum compressive strain acting on Mo–Mo bonds increases from 1.5% in Segment I to 2.2% in Segment II and Segment III for $2V_{S_t}$ (Fig. 3). The effect of S-vacancies on the buckling height is summarized in Table I.

To the extent that the lines of vacancies can be interpreted as simple models of twin or grain boundaries,[5,29] our calculations suggest that such formations will be pinned to ripplocations.

C. Defect-related electronic states

To obtain insights into the effect of the ripplocation on the electronic structure of single-layer MoS_2, we consider the density of states, for three different structural models: (a) a stoichiometric flat layer of MoS_2 [labeled "pristine" in Fig. 4(a)], (b) a stoichiometric flat layer uniformly strained along the zigzag direction ("strained"), and (c) a layer with a ripplocation ("rippled"). The strain in the compressed flat layer is 5.4%. We elected a relatively high value for strain to simulate the material near the point where it actually starts breaking as a limiting case. In all cases, we find little variation in the fundamental bandgap and no defect-related states in it. The bandgap increases after introducing strain to 1.76 eV (a 0.08 eV increase with respect to this of the stoichiometric flat layer, which has a gap of 1.68 eV), and a ripplocation to 1.82 eV (an increase of 0.14 eV). Fabbri *et al.*[19] reported an emission peak in the CL

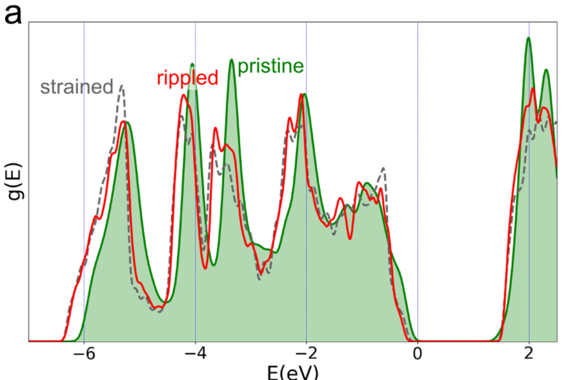

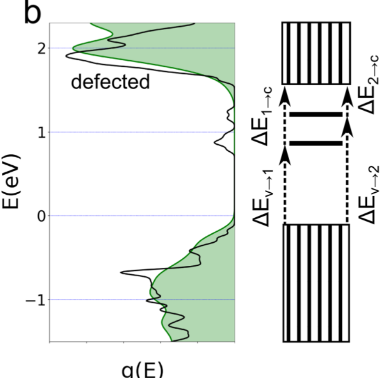

FIG. 4. (a) Electronic density of states, g(E), of the pristine flat and uncompressed (green), flat and compressed (5% strain; black), and rippled (red) structure of MoS_2. Zero (0) on the energy-axis denotes the valence band maximum of pristine flat MoS_2. (b) Electronic density of states, g(E), near the bandgap edges for pristine flat and for MoS_2 with a pair of S-vacancies. The schematic defines energies associated with transitions between the bandgap edges and gap states for $2V_S$ (see Table II).

Published under license by AIP Publishing.

TABLE II. Energies (in eV) associated with transitions between bandgap edges and defect-related states in S-deficient rippled MoS_2 [see also Fig. 4(b)].

	$2V_{S_t}$			$2V_{S_b}$		
	I	II	III	I	II	III
$v \rightarrow 1$	0.82	0.98	0.96	1.03	0.86	0.81
$1 \rightarrow c$	1.03	1.03	1.03	1.03	1.07	1.04
$v \rightarrow 2$	1.18	1.34	1.34	1.39	1.28	1.20
$2 \rightarrow c$	0.67	0.67	0.65	0.67	0.65	0.65

spectrum of rippled MoS_2 at 0.98 eV, but its origin could not be determined with certainty. Because we find that neither the ripplocation defect nor strain in the layer alone gives rise to defect-related states in the intrinsic bandgap, the origin of the observed emission peak cannot be attributed solely to atomic-scale ripples (or associated crystallographic dislocations). On the other hand, those authors report deficiency in sulfur in the sample, which in the light of our theoretical findings suggests that the observed feature in the CL spectrum is more likely to be the signature of S-vacancies.

To quantify the effect of S-vacancies on the electronic structure of the material, we calculate the minimum Kohn-Sham bandgap for defected structures of single-layer MoS_2 with two S-vacancies in the ripplocation (this corresponds to 3.6% concentration in defects). The energies associated with transitions between the bandgap edges and defect-related states for a pair of S-vacancies in the top or bottom atomic layer [Fig. 4(b)] are summarized in Table II for the three segments. As shown in Fig. 4(b), two S-vacancies in the ripplocation introduce defect states in the bandgap regardless of the curvature of the ripplocation within each Segment. We find that the position of defect-related states vary little among the different structural models: a defect-related state is found between 0.81 eV and 1.03 eV higher in energy than the valence band maximum (VBM), and another with energy in the range of 1.03–1.07 eV below the conduction band minimum (CBM). For comparison, a neutral S-vacancy in unstrained and flat single-layer MoS_2 is 1.3 eV above the VBM (0.3 eV below the CBM) and shifts to 1 eV above the VBM (0.3 eV below the CBM) under 1% compressive strain.[6] The defect-related states have a majority contribution from the Mo 4d orbitals and S 3p orbitals, as determined by projections of the layer's electronic states on the atoms orbitals, in agreement with previous work.[15] In the case of a pair of lines of S-vacancies, we identify multiple states in the bandgap with energies in wide range of 0.3–1.5 eV, including states with energies very close to those associated with a pair of S-vacancies. Miró *et al.*[30] studied transport effects in rippled MoS_2 and reported a decrease in electron conductance due to the presence of ripplocations. We expect that the presence of S-vacancies will increase scattering due to mid-gap states and further quench electron transport.

IV. CONCLUSIONS

We carried out first-principles calculations to investigate S-deficient forms of a free-standing single layer of MoS_2 with a ripplocation. We modeled deficiency in sulfur by S-vacancies and we quantified their effect on the structural and electronic structure properties of the material. Our estimates of formation energies of S-vacancies in the ripplocation are on average lower (by about 0.5–1.5 eV) than those reported in Ostadhossein *et al.*[24] The discrepancy could be attributed to differences primarily in the structural models and also the accuracy of methods used (reactive force field with multiple energy terms in the aforementioned work). The trends in the formation energy of S-vacancies with respect to the curvature of the ripplocation in the vicinity of the defects, however, are in qualitative agreement.

Strain induced by S-vacancies generally depend on the local curvature of the ripplocation, or, conversely, the distance between the vacancy and the center of the ripplocation. As a general rule, bonds near the S-vacancies compress, whereas a ripplocation alone compresses some interatomic distances (Mo−Mo and S_t−S_b bonds) and increases others (Mo−S_t and Mo−S_b). Our detailed calculations suggest that the emission peak in the CL spectrum at 0.98 eV reported in Fabbri *et al.*[19] is not due either to the ripplocation or to strain alone as they do not induce electronic states in the bandgap of MoS_2. The energy levels in the bandgap associated with S-vacancies, however, are in accordance with these experimental measurements. Therefore, the observed emission peak is more likely related to emerge from electronic transitions involving defect-related states and the bandgap edges, in the presence of ripplocations.

In DFT-based electronic structure calculations, the fundamental bandgap of semiconductors and insulators is underestimated. Furthermore, since DFT is a ground-state theory, excitonic effects, which can be particularly pronounced in the case of two-dimensional materials, are neglected in the calculation of optical transitions. Interestingly, the DFT correction for the bandgap, as obtained from more elaborate calculations, is approximately equal to the exciton binding energy, a mere numerical coincidence.[10] Accordingly, we expect that the trends we identified give a reasonable reference for spectroscopic observations. Our specific findings collectively aim to provide insights into the electronic structure of experimentally relevant forms of MoS_2 and to establish reliable reference information and structure-property relationships for the design of MoS_2-based materials for quantum devices.

ACKNOWLEDGMENTS

The authors would like to thank Venkataraman Swaminathan and Daniel Larson for helpful discussions. S.S. acknowledges support by the ARO MURI (Award No. W911NF14-0247). This work was supported by the DOE BES Award No. DE-SC0019300. For calculations, computational resources were used on the Odyssey cluster, which is maintained by the FAS Research Computing Group at Harvard University, and the Extreme Science and Engineering Discovery Environment (XSEDE), which is supported by the National Science Foundation (NSF) under Grant No. ACI-1053575.

REFERENCES

[1] A. Hashimoto, K. Suenaga, A. Gloter, K. Urita, and S. Iijima, Nature **430**, 870 (2004).
[2] S. N. Shirodkar and U. V. Waghmare, Phys. Rev. B **86**, 165401 (2012).
[3] F. Banhart, J. Kotakoski, and A. V. Krasheninnikov, ACS Nano **5**, 26 (2011).
[4] S. Tongay, J. Suh, C. Ataca, W. Fan, A. Luce, J. S. Kang, J. Liu, C. Ko, R. Raghunathanan, J. Zhou, F. Ogletree, J. Li, J. C. Grossman, and J. Wu, Sci. Rep. **3**, 2657 (2013).

Downloaded from http://pubs.aip.org/aip/jap/article-pdf/doi/10.1063/1.5099496/13866432/084303_1_online.pdf

Published under license by AIP Publishing.

[5]W. Zhou, X. Zou, S. Najmaei, Z. Liu, Y. Shi, J. Kong, J. Lou, P. M. Ajayan, B. I. Yakobson, and J.-C. Idrobo, Nano Lett. **13**, 2615 (2013).
[6]M. G. Sensoy, D. Vinichenko, W. Chen, C. M. Friend, and E. Kaxiras, Phys. Rev. B **95**, 014106 (2017).
[7]B. Radisavljevic, A. Radenovic, J. Brivio, V. Giacometti, and A. Kis, Nat. Nanotechnol. **6**, 147 (2011).
[8]Q. H. Wang, K. Kalantar-Zadeh, A. Kis, J. N. Coleman, and M. S. Strano, Nat. Nanotechnol. **7**, 699 (2012).
[9]K. F. Mak, K. He, J. Shan, and T. F. Heinz, Nat. Nanotechnol. **7**, 494 (2012).
[10]R. K. Defo, S. Fang, S. N. Shirodkar, G. A. Tritsaris, A. Dimoulas, and E. Kaxiras, Phys. Rev. B **94**, 155310 (2016).
[11]M. Koperski, K. Nogajewski, A. Arora, V. Cherkez, P. Mallet, J.-Y. Veuillen, J. Marcus, P. Kossacki, and M. Potemski, Nat. Nanotechnol. **10**, 503 (2015).
[12]M. Bernardi, M. Palummo, and J. C. Grossman, Nano Lett. **13**, 3664 (2013).
[13]R. R. Nair, P. Blake, A. N. Grigorenko, K. S. Novoselov, T. J. Booth, T. Stauber, N. M. R. Peres, and A. K. Geim, Science **320**, 1308 (2008).
[14]A. Splendiani, L. Sun, Y. Zhang, T. Li, J. Kim, C.-Y. Chim, G. Galli, and F. Wang, Nano Lett. **10**, 1271 (2010).
[15]H. Qiu, T. Xu, Z. Wang, W. Ren, H. Nan, Z. Ni, Q. Chen, S. Yuan, F. Miao, F. Song, G. Long, Y. Shi, L. Sun, J. Wang, and X. Wang, Nat. Commun. **4**, 2642 (2013).
[16]S. Najmaei, J. Yuan, J. Zhang, P. Ajayan, and J. Lou, Acc. Chem. Res. **48**, 31 (2015).
[17]H.-P. Komsa and A. V. Krasheninnikov, Phys. Rev. B **91**, 125304 (2015).
[18]D. Vinichenko, M. G. Sensoy, C. M. Friend, and E. Kaxiras, Phys. Rev. B **95**, 235310 (2017).
[19]F. Fabbri, E. Rotunno, E. Cinquanta, D. Campi, E. Bonnini, D. Kaplan, L. Lazzarini, M. Bernasconi, C. Ferrari, M. Longo *et al.*, Nat. Commun. **7**, 13044 (2016).
[20]H.-P. Komsa, J. Kotakoski, S. Kurasch, O. Lehtinen, U. Kaiser, and A. V. Krasheninnikov, Phys. Rev. Lett. **109**, 035503 (2012).
[21]H. Nan, Z. Wang, W. Wang, Z. Liang, Y. Lu, Q. Chen, D. He, P. Tan, F. Miao, X. Wang, J. Wang, and Z. Ni, ACS Nano **8**, 5738 (2014).
[22]M. M. Ugeda, A. J. Bradley, S.-F. Shi, F. H. da Jornada, Y. Zhang, D. Y. Qiu, W. Ruan, S.-K. Mo, Z. Hussain, Z.-X. Shen, F. Wang, S. G. Louie, and M. F. Crommie, Nat. Mater. **13**, 1091 (2014).
[23]A. Kushima, X. Qian, P. Zhao, S. Zhang, and J. Li, Nano Lett. **15**, 1302 (2015).
[24]A. Ostadhossein, A. Rahnamoun, Y. Wang, P. Zhao, S. Zhang, V. H. Crespi, and A. C. T. van Duin, J. Phys. Chem. Lett. **8**, 631 (2017).
[25]T. T. Tran, K. Bray, M. J. Ford, M. Toth, and I. Aharonovich, Nat. Nanotechnol. **11**, 37 (2016).
[26]P. Giannozzi, S. Baroni, N. Bonini, M. Calandra, R. Car, C. Cavazzoni, D. Ceresoli, G. L. Chiarotti, M. Cococcioni, I. Dabo, A. Dal Corso, S. de Gironcoli, S. Fabris, G. Fratesi, R. Gebauer, U. Gerstmann, C. Gougoussis, A. Kokalj, M. Lazzeri, L. Martin-Samos, N. Marzari, F. Mauri, R. Mazzarello, S. Paolini, A. Pasquarello, L. Paulatto, C. Sbraccia, S. Scandolo, G. Sclauzero, A. P. Seitsonen, A. Smogunov, P. Umari, and R. M. Wentzcovitch, J. Phys. Condens. Matter **21**, 395502 (2009).
[27]D. Vanderbilt, Phys. Rev. B **41**, 7892 (1990).
[28]J. P. Perdew, K. Burke, and M. Ernzerhof, Phys. Rev. Lett. **77**, 3865 (1996).
[29]H.-P. Komsa and A. V. Krasheninnikov, Adv. Electron. Mater. **3**, 1600468 (2017).
[30]P. Miró, M. Ghorbani-Asl, and T. Heine, Adv. Mater. **25**, 5473 (2013).

Downloaded from http://pubs.aip.org/aip/jap/article-pdf/doi/10.1063/1.5099496/13866432/084303_1_online.pdf

Published under license by AIP Publishing.